International Journal of Applied Ceramic Technology, Volume 5, Number 1, January 2008 , pp. 29-36(8)

http://dx.doi.org/10.1111/j.1744-7402.2008.02180.x

Low Temperature Processing of Dense Hydroxyapatite-Zirconia Composites

Y. Nayak, R. P. Rana, S.K. Pratihar, S. Bhattacharyya*.

Department of Ceramic Engineering, National Institute of Technology, Rourkela-769008, India

Abstract

Hydroxyapatite (HA) – YTZP (2, 5, 7.5 and 10 wt% ZrO_2) composite powders prepared from inorganic precursors were characterized by FTIR, DSC/TG, XRD and TEM. The calcined powders had HA and t / c-ZrO_2 which undergo structural changes between 650-1050^oC. TEM of calcined powder show larger HA particles (100nm) and smaller ZrO_2 particles (≤ 50nm). HA and HA -2 wt% ZrO_2 sintered samples had 98% density and it was (90-95%)) for HA – 5, 7.5 and 10 wt% ZrO_2. The bending strength of HA - 2wt% ZrO_2 composites was 72 MPa. The grain sizes of HA show a refinement with ZrO_2 addition.

Keywords: Dense-Hap: FTIR: Compressive: Strength: TZP

*corresponding author; mail id:santanub@nitrkl.ac.in

Introduction

Hydroxyapatite (HA) ceramics have widespread applicability in the biomedical field partially for repair or replacement of bone tissues. Owing to low strength and toughness of HA, its use is limited mainly to the non-load bearing components, e.g., small unloaded or low loaded implants, coating on metal implants and as bioactive filler powder or as a second phase in polymer based composites[1- 3]. For load bearing applications, the research on the use of HA as bioactive filler in ceramic and metallic matrix composites did not succeed due to the deleterious reactions taking place between HA and the matrix phase [4-6]. However, the use of HA in load bearing parts can be explored provided the strength and toughness of HA can be increased [7]. Among many oxide reinforcements, ZrO_2 is an important one, which has been used to increase the strength and toughness of Al_2O_3, mullite, spinel and many other ceramic materials. High sintered density and ultra fine particles (in the nano range) along with the use of stabilizers will ensure ZrO_2 mostly in tetragonal phase leading to improved mechanical properties of the composites. A number of approaches have been tried to prepare HA - ZrO_2 composites containing higher fraction of ZrO_2 (20-40 vol%) [8-11]. In these composites, the major problem encountered were the densification of the composites and the decomposition of HA to TCP [9]. Actually, the decomposition of HA to TCP is accelerated at the higher sintering temperatures (>1300^oC). With ZrO_2 addition the decomposition temperature is further lowered (in the range 1000^0C -1050^0C) [10]. Efforts to achieve densification at lower sintering temperature involved hot pressing/ hot isostatic pressing [11], spark plasma sintering [7] and use of additives (CaF_2) [8]. All the above composites in the HA – ZrO_2 system involved high volume fraction of ZrO_2 addition. On the other hand, the available literature on the processing, densification behaviour and mechanical properties of HA - ZrO_2 composites containing low volume fraction of ZrO_2 (≤20 vol%) is comparatively fewer in number [8,12,13]. Kim et al [8] studied the effect of calcium fluoride addition on

the reaction sintering and mechanical properties of HA-ZrO_2 composites containing 20vol% ZrO_2. Addition of CaF_2 promoted densification as well as retarded the HA to TCP decomposition. The densification temperature also decreased with CaF_2 addition. Highest flexural strength was 125 MPa and fracture toughness was 2 $MPam^{1/2}$, which were higher than pure HA. Pyda et al [12] studied the effect of chemical composition and morphology of zirconia particles on properties of HA-ZrO_2 particulate composites containing 11.9 vol% Ca or Y-stabilized ZrO_2. The composites were hot pressed in the temperature range 1150-1250^oC in an argon atmosphere. It was observed that isometric ZrO_2 crystallites incorporation in HA matrix increased both strength (180MPa) and toughness (1.1$MPam^{1/2}$) which were higher than pure HA. Ahn et al [13] studied the effect of nano zirconia reinforcement on the strength of hot pressed HA - ZrO_2 composites containing 1.5 to 8 wt% ZrO_2. They observed the highest strength and hardness at 3wt% ZrO_2 which subsequently decreased on higher ZrO_2 loading. They also reported that lower volume fraction of ZrO_2 addition will help to retain both HA and t-ZrO_2 phase, which may be due to the combined effect of matrix constraint and uniform dispersion of fine zirconia particles. Thus, it is expected that HA -ZrO_2 composites containing lower volume fraction of t-ZrO_2 may provide transformation toughening effect which can lead to improved mechanical properties of hydroxyapatite–zirconia composites [7, 8, 12-17].

The aim of the present investigation is to observe the effect of low volume percent TZP addition on the density, strength and microstructure of HA-ZrO_2 composites and an attempt has also been made to analyze the observed results with respect to phase analysis and microstructure of the samples for different HA-ZrO_2 composites. The exact effect of ZrO_2 addition (both at low and high ZrO_2 loading) cannot be understood unless a systematic investigation in this system is carried out.

Experimental:

The hydroxyapatite – zirconia composite preparation consisted of two parts:

(a) Preparation of nano TZP (2.5 mol% Y_2O_3) powder using precipitation method and

(b) Preparation of hydroxyapatite zirconia composite (containing 2, 5, 7.5 and 10 wt% TZP) by reverse strike precipitation method which are denoted as HZ2, HZ5, HZ7, HZ10 respectively.

The precursors used for TZP (2.5 mol% Y_2O_3) were $ZrOCl_2.8H_2O$ (Loba Chemicals, India) and Y_2O_3 (Indian Rare Earths Limited, India). The concentration of $ZrOCl_2$ solution was 0.75 moles/liter in which requisite amount of Y_2O_3 powder was dissolved. Precipitation was carried out using NH_4OH (1:1) (Oster Chemicals, India) solution at pH 10. The precipitates were water washed to remove chloride ions followed by drying and calcination at 850^oC/2h to obtain TZP powder. The out line of the powder preparation steps are shown in Fig. 1(a).

The HA-ZrO_2 composite powders were prepared from equimolar aqueous solution (1.63 mol/liter) of both $Ca(NO_3)_2.2H_2O$ (Oster Chemicals, India) and $(NH_4)_2HPO_4$ (Nice Chemicals, India).These two solutions were mixed together along with the addition of few drops on HNO_3 to get a colourless solution. In the usual method of HA-ZrO_2 composite powder preparation, NH_4OH is added to the above mixed solution. However, in the present investigation, the mixed solution was drop wise added to a beaker containing calcined Y-TZP dispersed in NH_4OH, while the beaker was being vigorously stirred. This allowed better and uniform reaction of $Ca(NO_3)_2$ and $(NH4)_2HPO_4$ with NH_4OH and for the present investigation, this precipitation process has been termed as “reverse strike precipitation” method. The outline of the precipitation process is shown in Fig.1(b). The as precipitated amorphous powders having varying proportion of ZrO_2 were subjected to hot water and propanol washing to prevent particle agglomeration on

drying of these powders. It has been reported that the presence of hydroxyl and other ions (e.g. Cl^-) affects the crystallization and densification behaviour of many ceramic powders [13]. The washed powders were oven dried for 24 h and. The FTIR spectra of the as dried precipitated powder of HA and HA-ZrO2 was observed in Perkin Elmer FTIR spectrophotometer (Spectrum RX-1). The spectrum was taken in KBr pellet mode in the wave number range 4400-400cm^{-1}. A small part of the dried powder was subjected to thermal analysis in DSC/TG mode (Netzsch 402 C) till 1200^oC at a heating rate of 10^oC/min in air. The dried powders were calcined in different temperature range from 650^oC to 850^oC/2h in air. The phase analysis of the calcined powders and sintered pellets was studied by XRD (Philips PW1830 Holland). The relative amount of the different phases present in the sintered pellet was calculated from the relative XRD peak intensities of the different phases. The particle morphology was studied by TEM (Philips CM 200). The densification behaviour was studied in a dilatometer (Netzsch DL 402 C). The powders were uniaxially compressed at 280 MPa using 3 wt% PVA as binder. The density of the sintered samples was measured by Archimedes principle using kerosene as the immersion liquid. The strength of the sintered composites were measured in three point bending (span length = 20mm) as well as in diametral compression of the cylindrical disk (12.5 mm diameter) at a crosshead speed of 0.2 mm/min. The microstructures of the sintered and polished pellets were studied by SEM (JSM-6480LV). In all the above characterization of HA-ZrO_2 composite, HA was used as the control sample.

Results and discussion:

FTIR

The FTIR spectra of pure HA (Fig. 2) shows all the peaks corresponding to $(OH)^-$ and $(PO_4)^{-3}$ stretching and no extra peak was observed. The broad peak between 3750 and

2900 cm^{-1} corresponds to the hydrogen bonded O-H group stretch of Hap and water. Thus the processed HA was stochiometric. The three strong peaks at around 1060 cm^{-1}, 570 and 606 cm^{-1} attributes to the P-O vibration modes. The band at 570 and 606 cm^{-1} corresponds to the bending mode of $(PO_4)^{3-}$ and the strong band at 1060 $cm^{-1}$and 963 cm^{-1} are due to the vibration of $(PO_4)^{3-}$ group. The absence of broadening of the peak at 1060 cm^{-1} further confirms no decomposition of HA to β–TCP at 850^oC. The decrease in broadness of the peak between 3750 and 2900 cm^{-1} with the increase in calcinations temperature indicates the removal of absorbed H_2O.

DSC/TG

The DSC/TG curve of the precipitated powders of HA is shown in Fig. 3 (a). The curve shows a total weight loss of 5.78%, which takes place in two stages, It has a broad but sharp endothermic peak in the temperature range 30-100^oC with a peak at 70^oC. This endothermic peak is associated with a weight loss of 3.55%, which could be related to the loss of adsorbed water from HA. Following this peak, there is broad and diffused exothermic peak in the temperature range 250-400^oC. This exothermic peak also shows a gradual weight loss of about 2.23 %. X-ray diffraction of the precipitated powder heated at 400^oC shows peaks corresponding to HA only. Thus this diffuse exothermic peak is due to the crystallization of HA from the precipitated amorphous powder.

Figure 3 (b) shows the DSC/TG curve of the precipitated HZ2 powder. The nature of the curve and the total weight loss (4.74 %) is comparable with that of pure HA (5.78 %). This curve also shows one broad endothermic peak in the temperature range 30-100^oC with peak at about 70^oC along with a weight loss of 3.21 % corresponding to the loss of adsorbed water. The weight loss is lower than pure HA as the amount of HA is less by 2 %. Similarly, the second phase weight loss from 100^oC to 400^oC is also lower in HZ2 in comparison to pure HA. However, the exothermic peak of HZ2 is at a

lower temperature and it is sharper as compared to pure HA. This implies that the addition of ZrO_2 reduces the crystallization temperature and also improves the crystallization behaviour of HA. However, no further change in either the crystallization behaviour or the crystallization temperature could be observed in HA with still higher amount of TZP (viz.HZ5, HZ7 and HZ10) samples.

Further, the DSC/TG curve of both HA and HA-ZrO_2 powders show a broad exothermic peak in the temperature range 800°C-1000°C. This exothermic peak is not associated with any weight loss. Therefore, the peak should correspond to phase changes/ordering in HA and/or ZrO_2. In order to validate the DSC curve, the position of the first three peaks of HA (or triplets) (d= 2.81A°, 2.72A°, 2.78A° respectively) were monitored as a function of calcination temperature. The results are shown in (Fig.4(b)), where the left hand pattern (Pattern A) shows the complete XRD profile of HA and HA-ZrO_2 composites, and the right hand pattern (Pattern B) is the "zoomed in" pattern of the same in the 2θ range 30-35° It is clear from the patterns that at 650°C the triplets are not well separated and only 2 peaks (d= 2.81A° ,2.72A°) are distinguishable. With increase in calcination temperature to 850°C, besides the above two, a third peak (as split peak) appears at d= 2.78. Finally, at 1050°C, all the three peaks could be clearly distinguished. It could also be seen from the zoomed in pattern, that the peak position shifts towards lower d value as well as the peak intensity and sharpness increases. Thus we can refer that at 650°C, HA is poorly crystallized (disorder state) and it becomes perfectly crystalline at 1050°C. This phase change from poorly crystallized HA to perfectly crystallize HA shows up a broad exothermic peak in the temperature 800°C-1000°C. Similar observation could be made from the XRD pattern of calcined HA-ZrO_2 powders. Moreover, the presence of ZrO_2 also contributes to exothermic peak because t-ZrO2 prepared from an amorphous powder undergoes the following phase change amorphous-cubic- tetragonal. It has been observed in our earlier study [18] that the

cubic-tetragonal phase change in ZrO_2 takes place around 850^oC. This could also be observed as exothermic peak in DSC. Thus in HA-ZrO_2 powder, we could observe two distinct peaks: one due to HA phase change and the other due to ZrO_2 phase change.

Phase analysis of calcined powder

Fig. 4(a) shows the XRD pattern of calcined HA and HA–TZP (HZ2, HZ5, HZ7, HZ10) composite powder calcined at 850^oC. The pattern shows that HA is stable up to 850^oC. The t-ZrO_2/c-ZrO_2 peaks could be detected from HZ2 in ZrO_2 containing samples (HZ2 to HZ10). The intensity of ZrO_2 peak increases at higher ZrO_2 content. No other phases like TCP, $CaZrO_3$ or m-ZrO_2 could be detected. As discussed in the DSC/TG section, with the increase in calcination temperature the'd' value of HA peaks shift to lower value (Fig.4(b)). From the XRD pattern, it is clear that in the calcined powder only HA and t-ZrO_2 is present. No other phases like TCP, $CaZrO_3$ or m–ZrO_2 could be detected. The intensity of t-ZrO_2 increases with the increase in wt% of zirconia addition.

Particle morphology of calcined powder

Fig. 5 (a, b) shows the TEM photograph of calcined HA and HZ2 powder respectively. The small and spherical particles are ZrO_2 while the lighter ones are HA It could be seen that HA particles are both spherical and cube shaped in the size range 50-100 nm. Mostly the ZrO_2 particles are seen on the surface of HA particles. Some clusters of ZrO_2 are also seen in the top part of the Fig .5(b).

Densification behaviour and phase analysis of sintered compacts

Fig 6 shows the nonisothermal sintering behaviour of HA and HZ2, HZ5, HZ7 and HZ10 composites. However, a significantly lower density is observed at 7.5 and 10 wt% TZP

additions. The reduction in densification at 7.5 and 10 wt% TZP resulted due to the higher sintering temperature of TZP which has a higher sintering temperature and hence could not be densified at 1250^{o}C. However, for HZ2 it appears that some other mechanism is playing a role in improving the densification. The relative sintered density at 1250^{o}C was given in Table-II. The XRD pattern (Fig. 6) shows phases in the sintered samples of HA and HZ2, HZ5, HZ7 and HZ10. The XRD pattern shows that beyond 2 wt% TZP additions, the sintered composites also contain $\beta-$TCP and $CaZrO_3$. In HZ2, although the shrinkage starts at nearly the same temperature as that of HA, HZ2 has higher shrinkage in comparison to HA. This implies that the sintered density of HA increases on addition of 2 wt% ZrO_2

Microstructural development on sintering

The HZ2, HZ5, HZ7 and HZ10 samples were sintered in air in the temperature range 1150^{o}C-1250^{o}C for 2 hours. The microstructure development of different HA-TZP composites as a function of varying TZP content were studied for samples sintered at the highest temperature. Fig 8 (a-c) shows the microstructure of different HA-TZP composites (a) HZ2, (b) HZ7, (c) HZ10. All these samples were sintered at 1250^{o}C for 4 hrs. For comparison, the microstructure of pure HA is also shown in Fig 8 (d) which shows a mixed grain size for HA. The larger grains of HA are in 4-6 μm, while the smaller grains are in the range 1-2 μm. Fig. 8 (a) shows that HZ2 samples has a dense microstructure with HA grains size in the range 2-4 μm, although some larger grains 5-6 μm could also be seen. The microstructure also contains void spaces and bright small grains (< 1μm) distributed in the matrix. It appears that many of these voids spaces have been created due to the pull out of ZrO_2 grains during specimen preparation. The microstructure of HZ7 (Fig-8(b)) clearly shows the effect of TZP addition on the grain

size distribution of HA. In this sample, though some large grains (~ 5μm) are present many small grains (1-2μm) could also be seen. The ZrO_2 pull out during polishing is evident and some ZrO_2 particles are also present as clusters. The microstructure is further refined in HZ10 (Fig.8(c)). Although this microstructure has a mixture of large grain size (~ 5μm) and very small grain (0.5μm), the distribution has become narrow. The bright cluster of ZrO_2 grains are seen near the multiple grain junctions. The microstructure (Fig 8(a)-8(c)) thus shows that addition of TZP to HA refine the grain size and produces an increased population of finer grains. However, the distribution of TZP is not uniform and it produces grain clusters. The TZP cluster size increases with increasing weight fraction of TZP. The effect of TZP addition on the grain size distribution is shown in Table I.

Mechanical properties

Table II lists the diametral compression as well as bending strength of sintered HA and HA-TZP composites. The Table shows that following the density trend the strength of HZ5, HZ7 and HZ10 decreases with increasing TZP content. However, the strength increases significantly for HZ2 composites. This is an interesting observation and needs much careful and detailed study. As already stated this study deals only with the effect of ZrO_2 addition on the density, strength and microstructure. The exact effect of low ZrO_2 addition needs detailed TEM analysis, which will be taken up in future study. Though the microstructure indicates grain refinement with TZP addition, the addition of TZP also increases the porosity due to incomplete densification due to the higher sintering temperature of TZP. Thus the mechanical properties decrease with increasing TZP content.

Conclusions

Hydroxyapatite and its composite with zirconia containing 2, 5, 7.5 and 10 wt% TZP were prepared by reverse strike precipitation method. DSC/TG study revealed that addition of TZP to HA lower the decomposition weight loss and promotes low temperature crystallization of HA. TEM analysis of calcined powders show spherical particles of TZP dispersed in cuboidal/ spherical HA grains. The sintered density of HA increases with 2 wt% TZP addition and it reduces with further addition of TZP. XRD revealed that in the sintered samples only HA and t-ZrO_2 were present for 2wt% TZP addition. For higher TZP content (5, 7.5 and 10 wt%) both $CaZrO_3$ as well as α-TCP could also be seen along with HA and t-ZrO_2. The bending strength of HA (35 MPa) increases to 70 MPa at 2 wt% TZP addition followed by a decrease at higher TZP content. SEM microstructures show a grain refinement of HA with TZP addition. The decrease in strength at higher TZP addition could be related to the improper densification of the composite at higher TZP loading.

References:

[1]L. L. Hench, “Bioceramics,” J. Am. Ceram. Soc., 81 [7]1705-28 (1998).

[2]L. L. Hench and J. Wilson, Science., 226 [11] 630- 636 (1984).

[3]G. De With, H. J. A. Van Dijk, N. Hattu, K. Prijs,”Preparation, microstructure and mechanical properties of dense polycrystalline hydroxyapatite,” J. Mater. Sci., 16 [6] 1592-1598 (1981).

[4]K. Ioku, S. Somiya, M. Yoshimura , ”Hydroxyapatite ceramics with tetragonal zirconia particles dispersion prepared by HIP postsintering,” J. Ceram. Soc. Jpn. Int. Ed., 99 [3] 196-203 (1991).

[5]M. Knepper, B. Milthrop, S. Moricca, ”Interdiffusion in short-fibre reinforced hydroxyapatite ceramics,“J. Mater. Sci. Mater. Med., 9 [10] 589-596 (1998).

[6]Y.- M. Kong, S. Kim, H.- E. Kim, ”Reinforcement of hydroxyapatite bioceramic by addition of ZrO_2 coated with Al_2O_3,”.J. Am. Ceram. Soc., 82 [11] 2963-68 (1999).

[7]Z. Shen, E. Adolfsson, M. Nygren, L. Gao, H. Kawaoka, K. Niihara,“Dense Hydroxyapatite-Zirconia Ceramic Composites with High Strength for Biological Application,” Adv. Mater., 13 [3]214 -16 (2001).

[8]H.- W. Kim, Y.-H. Koh, B.-H. Yoon, and H.-E. Kim,“Reaction sintering and mechanical properties of hydroxyapatite-zirconia composites with calcium fluoride addition,” J. Am. Ceram. Soc., 85 [6] 1634-36 (2002).

[9]J. Li, L. Hermansson and R. Soremark, “Synthesis and sintering of hydroxyapatite –zirconia composite,” J. Mater. Sci.: Mater. Med., 4 [1] 50-54 (1993).

[10]R. Ramachandra Rao and T. S. Kannan,“Synthesis and sintering of hydroxyapatite– zirconia composites,” Mater. Sci. Eng. C., 20 [1-2]187-93 (2002).

[11]J. Li, H. Liao and L. Hermansson,“Sintering of partially stabilized zirconia and partially stabilized zirconia-hydroxyapatite composites by hot isostatic pressing and pressureless sintering,” Biomaterials., 17 [18]1787-90 (1996).

[12]W. Pyda, A. Slosarczyk, Z. Paszkiewicz, A. Rapacz-Kmita, M. Haberko, A. Pyda, “Effect of Chemical Composition and Morphology of Zirconia Particles on Properties of HAp-zirconia Particulate Composites,“ Key Engineering Materials Vol., 206-213 pp.1567-1570(2002).

[13]E. S. Ahn, N. J. Gleason and J. Y. Ying,"The effect of zirconia reinforcing agents on the microstructure and mechanical properties of hydroxyapatite-based composites," J. Am. Ceram. Soc., 88 [12] 3374-3379 (2005).

[14]S. H Kim, H. C. Lee, H. G. Bang and S, Y. Park, "Effect of MgF_2 additive on the mechanical properties in hydroxyapatite/zirconia composites,"Materials Science Forum., Vols. 510-511 pp. 478- 481(2006).

[15] F. Mezahi, A. Harabi, S. Zouai, S. Achour and D. B. Assolant, "Effect of stabilized ZrO_2 , Al_2O_3 and TiO_2 on sintering of hydroxyapatite," Materials Science Forum., Vols. 492-493 pp. 241-246(2005).

[16] A. R. Kmita, A. Slosarczyk and Z. Paszkiewicz, "Mechanical properties of HAp–ZrO_2 composites," *J. Eur. Ceram. Soc.,* 26, pp.1481–1488(2006).

[17]C-Y.Chiu, H. C. Hsu and W. H. Tuan,"effect of Zirconia addition on the Microstructural evolution of porus hydroxyapatite," Ceramics International., 33.pp715-718 (2007).

[18]Raghunath P Rana, Swadesh K Pratihar and Santanu Bhattacharyya, "Effect of Powder Treatment on the Crystallization Behaviour and Phase Evolution of Al_2O_3-High ZrO_2 Nanocomposites," J. Mat. Science., 41, 7025-32(2006).

List of Figures and Tables

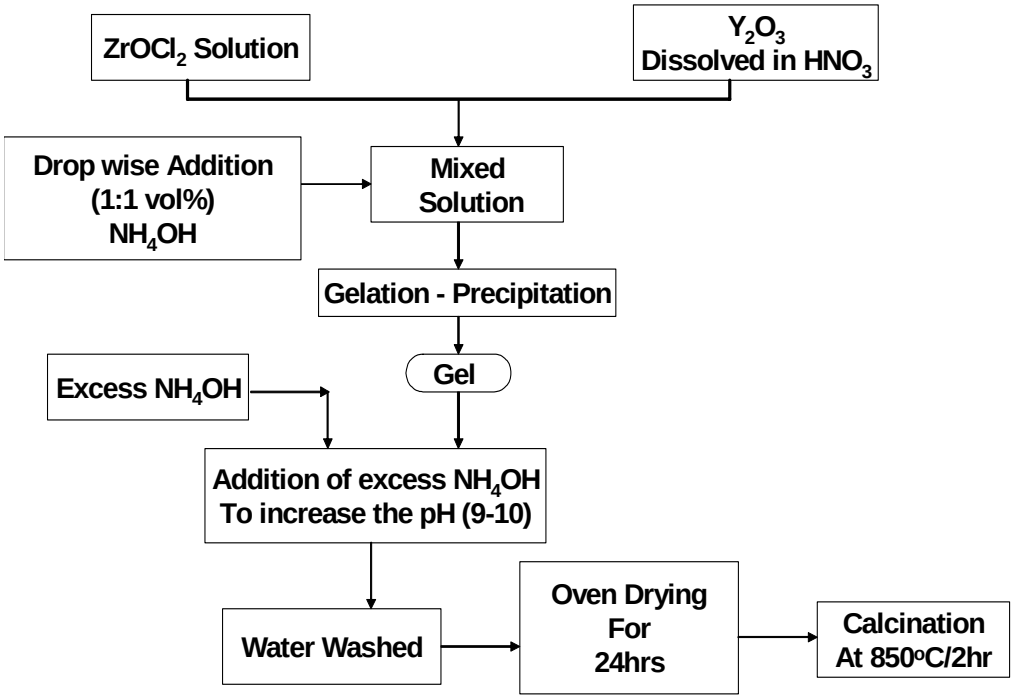

Fig. 1 (a) Flow Diagram for Synthesis of 2.5Y-TZP
(Y. Nayak et al)

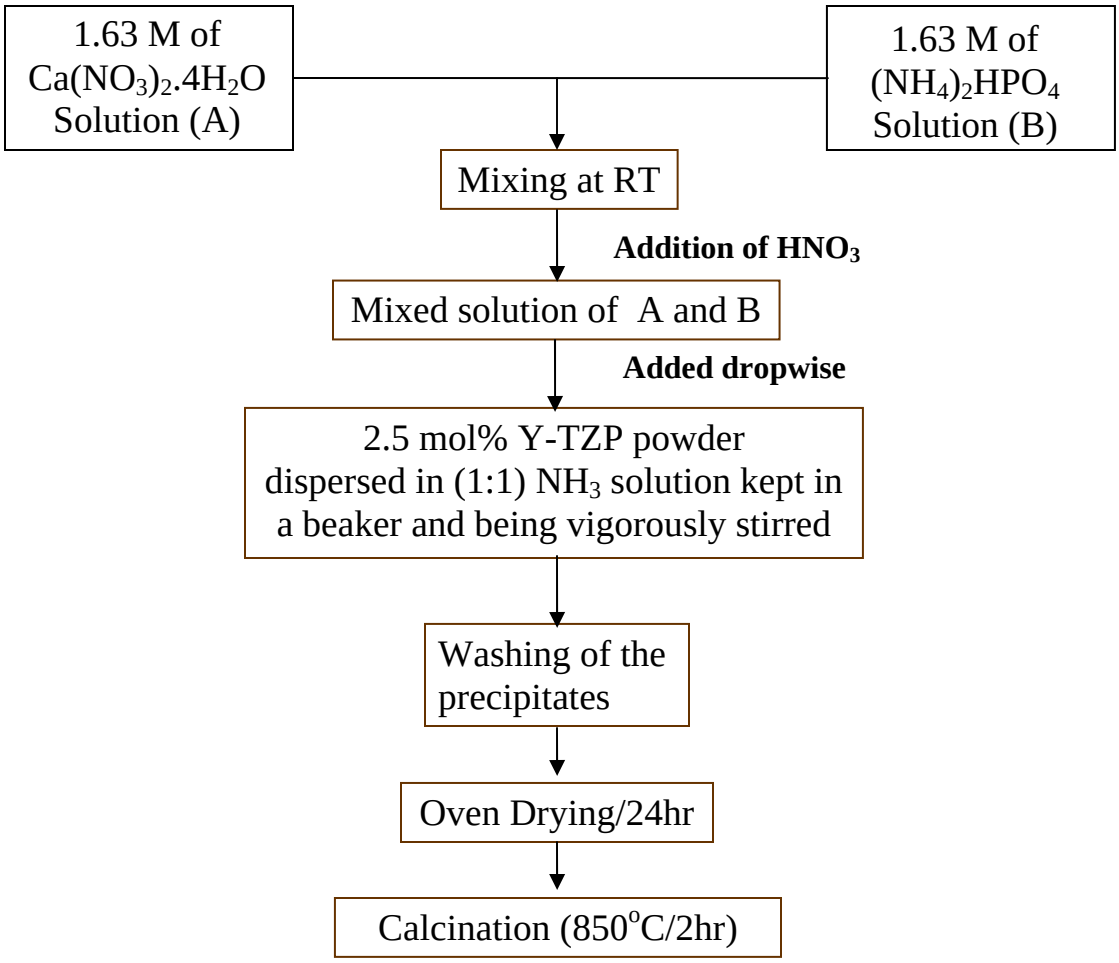

Fig. 1(b) Flow Diagram for Synthesis of HA- (2, 5, 7.5, 10 wt%)
(Y. Nayak et al)

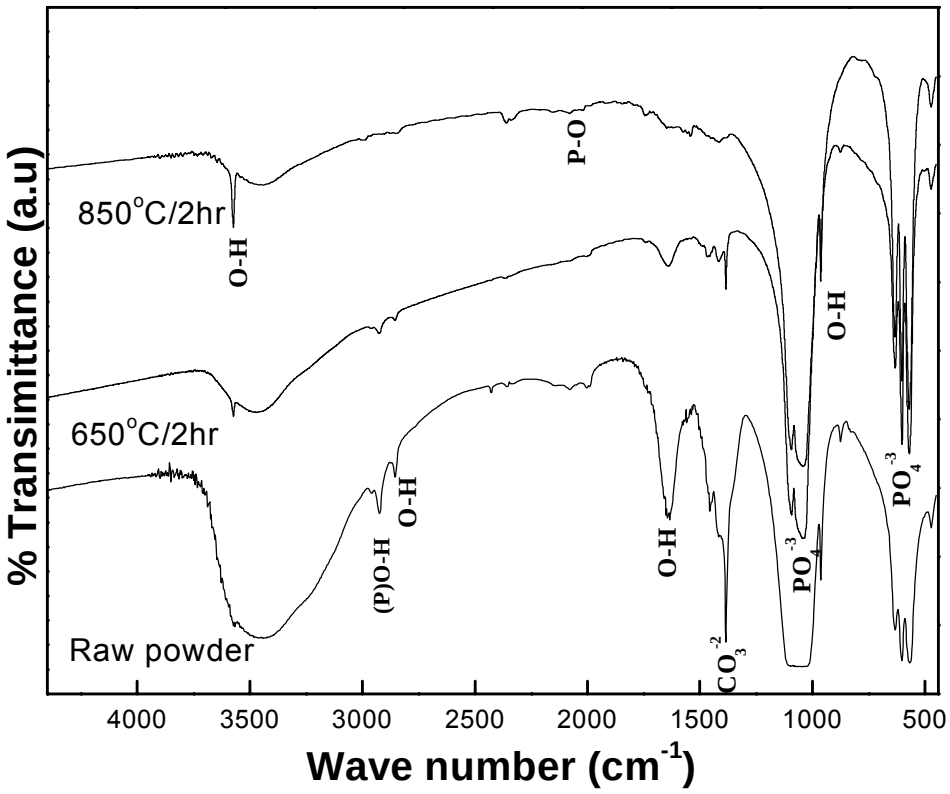

Fig. 2 FTIR Spectra of HA as a function of calcination temperature
(Y. Nayak et al)

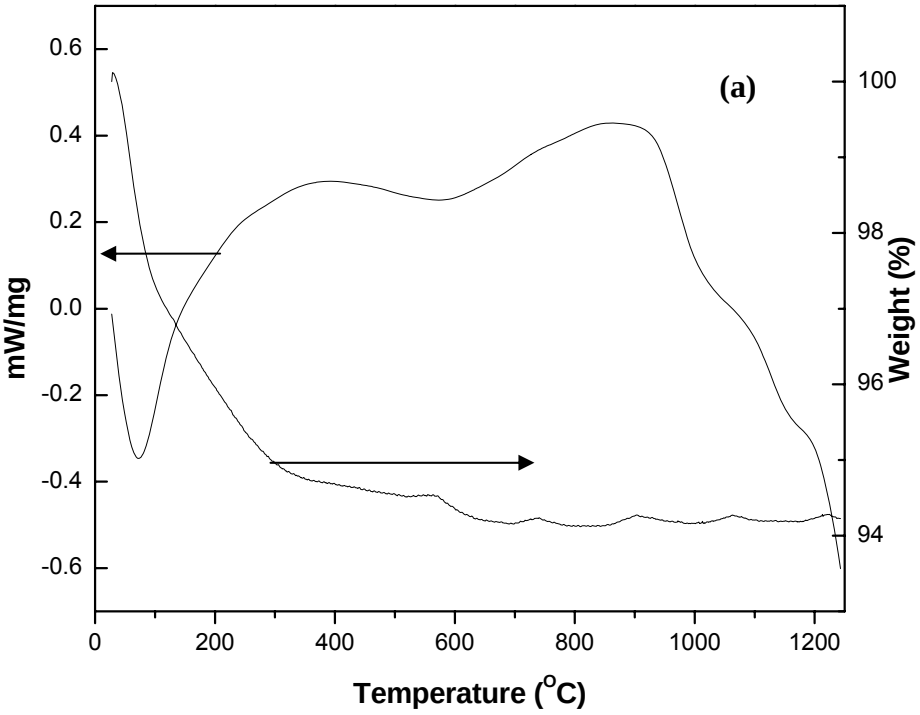

Fig. 3(a)DSC/TG curve of HA powder
(Y. Nayak et al)

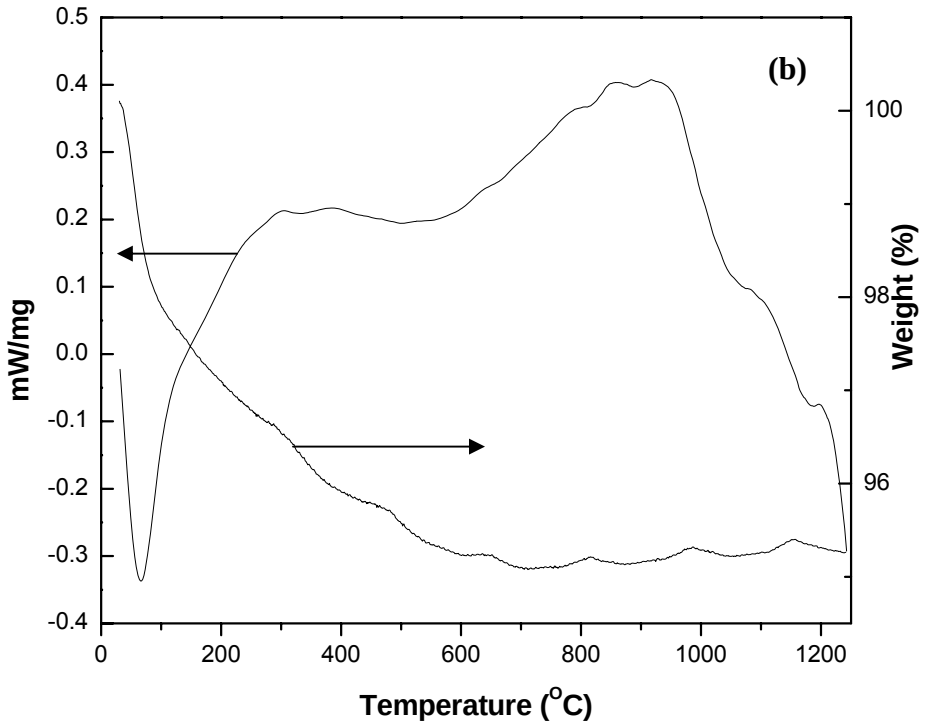

Fig. 3(b) DSC/TG curve of HZ2 powder
(Y. Nayak et al)

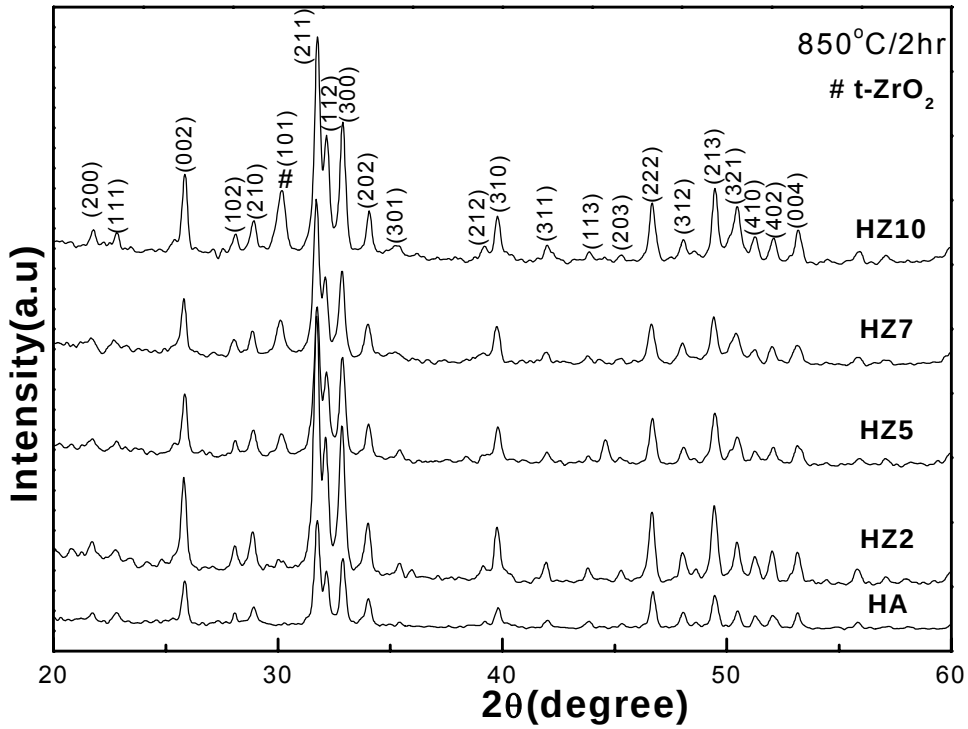

Fig. 4 (a) XRD analysis of HA, HA-ZrO_2 composite powder calcined at 850°C2hr
(Y. Nayak et al)

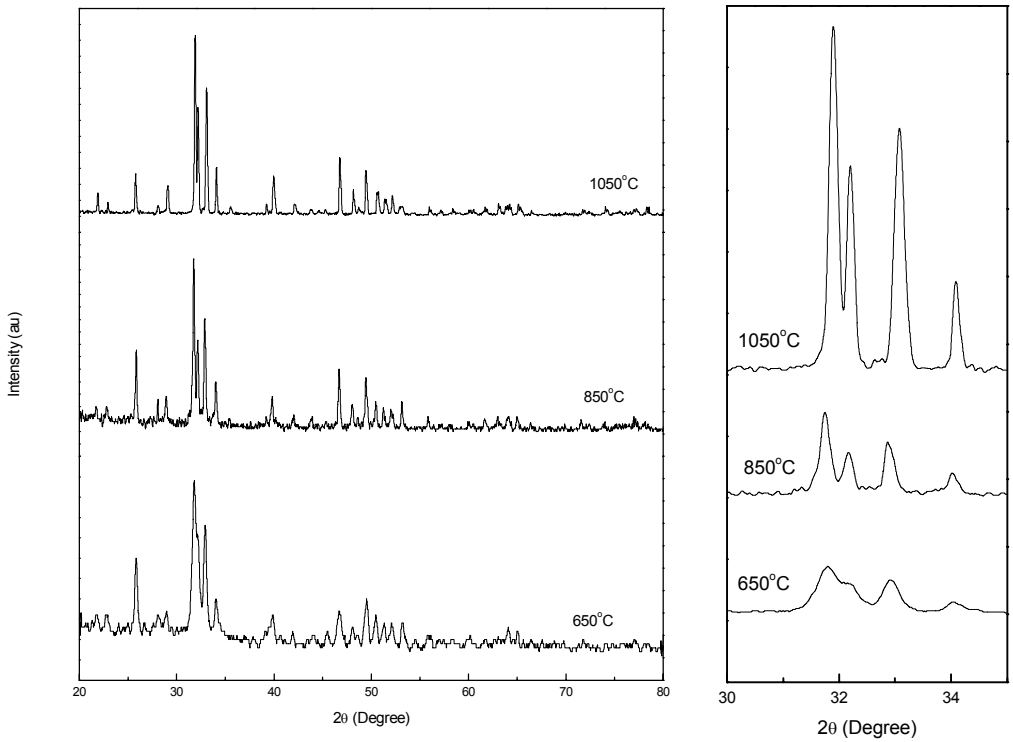

Fig. 4 (b) Expanded region of XRD pattern to show the peak shifting of HA.
(Y. Nayak et al)

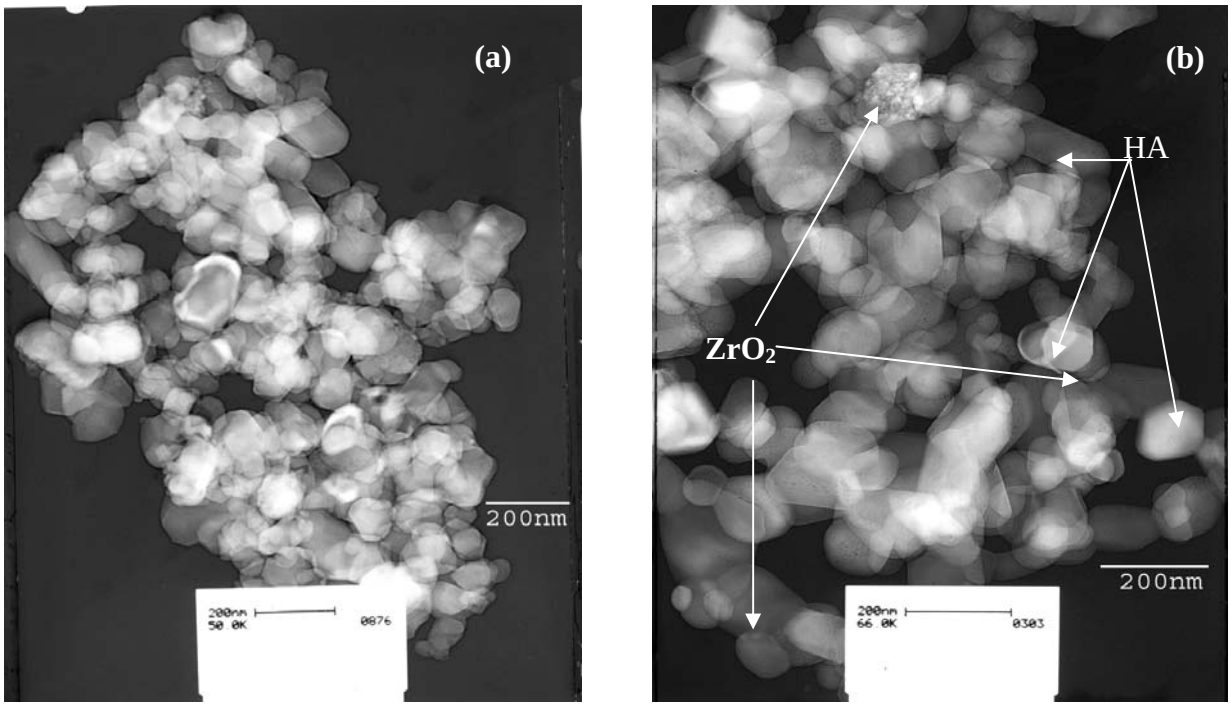

Fig. 5 TEM of (a) HA powder (b) HZ2 powder calcined at 850^{o}/2hr
(Y. Nayak et al)

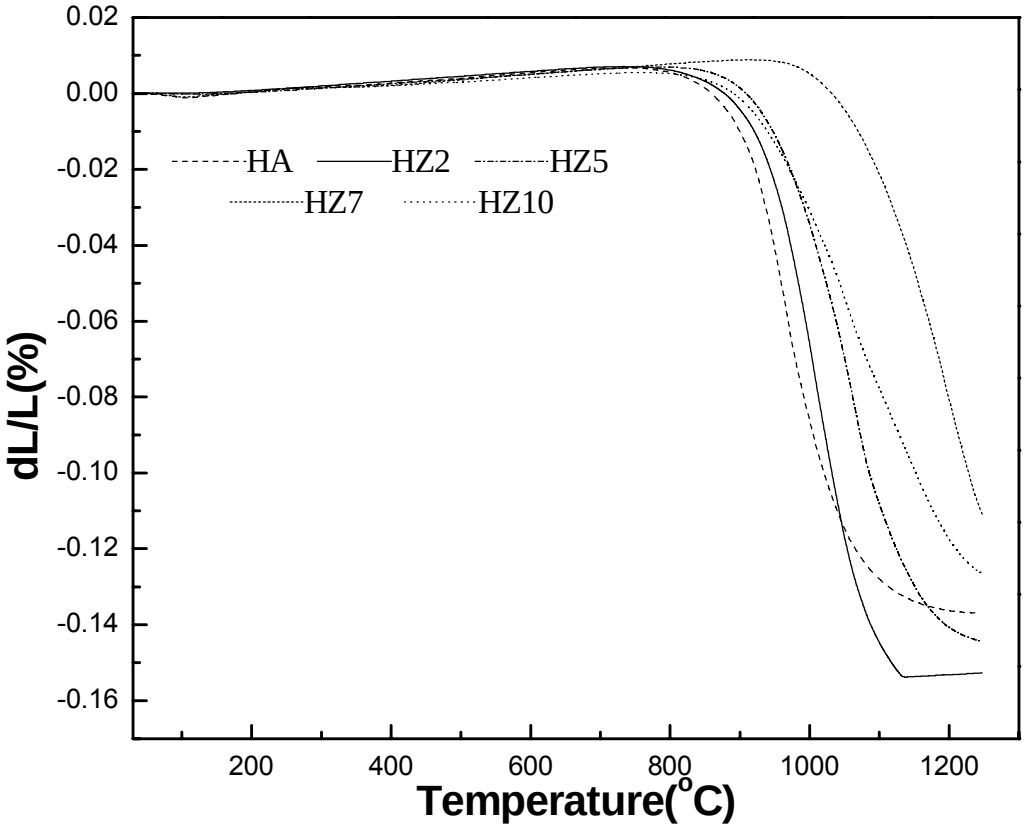

Fig. 6 Non isothermal densification curve of HA, HA-ZrO_2 composites
(Y. Nayak et al)

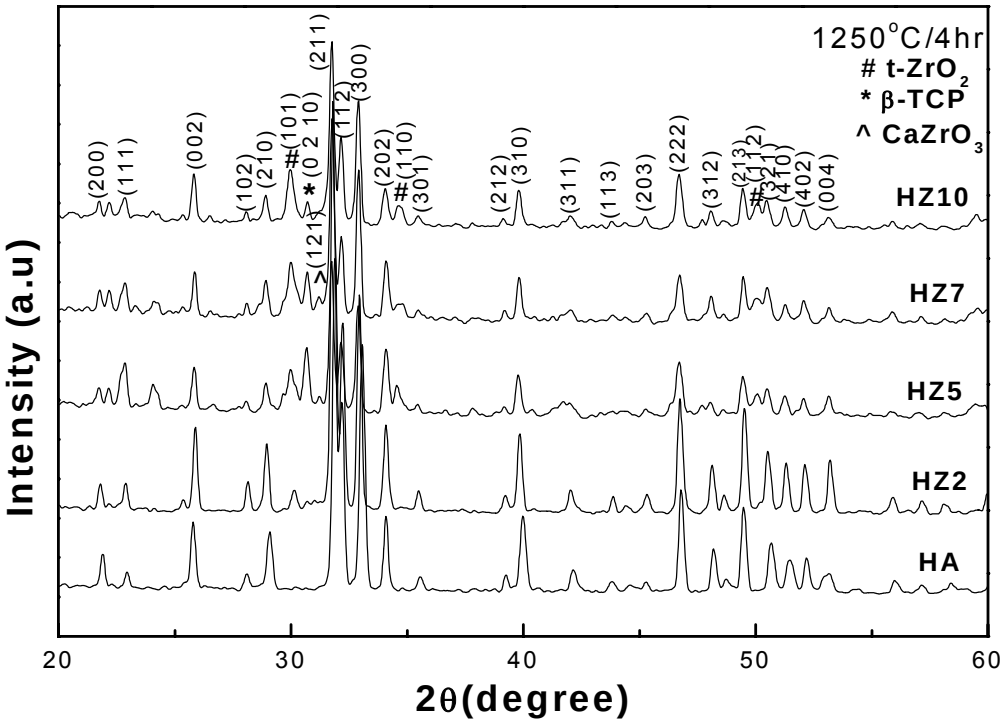

Fig. 7 XRD analysis of HA, HA-ZrO_2 composites sintered at 1250°C/4hr
(Y. Nayak et al)

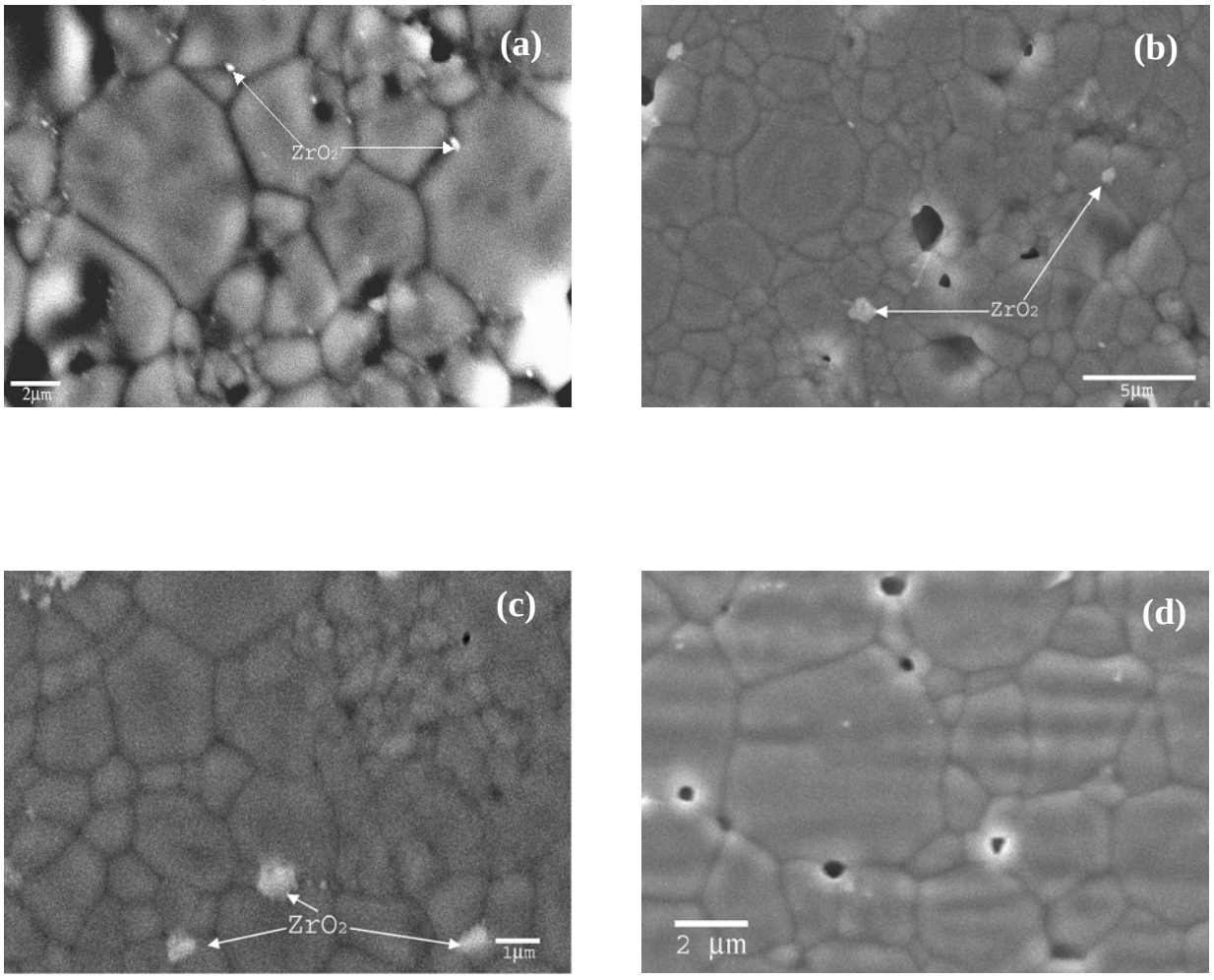

Fig. 8 SEM of HA, HA-ZrO_2 composites sintered at 1250^{o}C/4hr (a) HZ2, (b) HZ7, (c) HZ10 and (d) HA.

(Y. Nayak et al)

Grain Size (μm)	HA		HZ2		HZ7		HZ10	
	Coarse	Fine	Coarse	Fine	Coarse	Fine	Coarse	Fine
Average	3.63 ±1.15	1.13 ±0.3	3.64 ± 1.76	0.93 ± 0.36	2.70 ± 1.09	0.79 ± 0.39	1.57 ± 0.45	0.62 ± 0.24
Mean	2.48 ± 1.49		2.73 ± 1.94		1.50 ± 1.17		0.99 ± 0.57	

Table I Grain size distribution of HA, HA-ZrO_2 composites sintered at 1250^{o}C/4hr
(Y. Nayak et al)

Composition	Relative Sintered Density (%)	Diametral compression Strength (MPa)	Three point Bending Strength (MPa)	Phases in Sintered HA Sample (vol%)			
				HA	t-ZrO_2	CZ	TCP
HA	98.0	13.0 ±1.03	35 ±1.2	100	-	-	-
HZ2	99.6	34.5 ±2.763	72 ±3.6	96.50	3.50	-	-
HZ5	96.3	11.3 ± 1.04	31 ±1.55	64.9	11.3	6.2	17.6
HZ7	92.4	17.0 ±1.362	40 ±2	71.2	12.7	5.1	11
HZ10	90.0	13.0 ± 0.907	36 ±1.75	79	14.50	Tr.	6.5

Table II Density and mechanical properties of sintered compact of HA and HA-ZrO_2 composite

(Y. Nayak et al)